5-2013

A Novel Mechanism for Mechanosensing by Endothelial Cells

Jennifer MacDowell

University of Maine - Main

A NOVEL MECHANISM FOR MECHANOSENSING BY ENDOTHELIAL

CELLS

by

Jennifer MacDowell

A Thesis Submitted in Partial Fulfillment
of the Requirements for a Degree with Honors
(Biochemistry)

The Honors College

University of Maine

May 2013

Advisory Committee:
Sharon L. Ashworth, Assistant Research Professor of Cell Biology, Co-advisor
Alireza Sarvestani, Assistant Professor, Mechanical Engineering, Co-advisor
Mimi Killinger, Rezendes Preceptor for the Arts, Honors College
Dorothy E. Croall, PhD., Professor of Biochemistry
Robert Gundersen, Chair and Associate Professor of Molecular and Biomedical Sciences

ABSTRACT

The formation of new vasculature is an essential process, but can also be utilized by cancerous cells. Angiogenesis requires the directed migration of the endothelial cells lining the nascent blood vessels. This process is largely mediated by integrin, which plays a key role in the interplay between sensing a force in the extracellular matrix (ECM) and transducing this signal, a process termed mechanotransduction. Through cell-ECM focal adhesions, integrin mediates the signaling both into and out of the cell, promoting growth of focal adhesions and subsequent cell spreading and migration. In order to study focal adhesion dynamics related to force, we observed cells on three different substrates: polyacrylamide gels, polydimethylsiloxane (PDMS) micro pillars, and polyacrylamide gels containing fluorescent beads. The mobility of integrin on the different substrates was assessed using fluorescent recovery after photo-bleaching (FRAP) and analyzed along with cell traction force measurements. These studies serve to further the understanding of our knowledge of integrin and its role in mechanotransduction and migration. It will, therefore, aid in the advancement of both tissue engineering and cancer treatment research.

TABLE OF CONTENTS

ACKNOWLEDGEMENTS

LIST OF FIGURES

CHAPTER 1: INTRODUCTION

Angiogenesis, the process by which pre-existing blood vessels expand and create new vasculature, is essential for normal system functionality such as wound healing and development, but it is also crucial for tumor growth and metastasis. As cancer cells divide and grow, consuming all the oxygen and nutrients in their surrounding environment, they then require new vasculature in order to bring blood to the tumor. Cancer cells employ the same chemical and mechanical stimuli as non-cancerous cells in order to initiate the formation of new vasculature (Strömblad & Cheresh, 1996). Angiogenesis requires the directed migration of the endothelial cells lining the nascent blood vessels. Chemotaxis, the directed migration towards or away from a chemical concentration gradient, has been the focus of many studies (Swaney et al., 2010). These studies have shown that angiogenesis can be induced by chemotactic factors such as basic fibroblast growth factor (bFGF), transforming growth factor α (TGF-α) and vascular endothelial growth factor (VEGF) (Strömblad & Cheresh, 1996). While chemotactic factors do play an important role in cell migration, mechanical stimuli in the environment of a cell also affect cell adhesion, and therefore its migration. As endothelial cells begin to migrate during angiogenesis, they secrete matrix metalloproteinases (MMPs) to degrade the surrounding ECM (Strömblad & Cheresh, 1996). This remodelling of the environment around the cell alters the density or rigidity of the cell's substrate, thus altering the mechanical stimuli to the surrounding cells. Integrin, a trans-membrane heterodimer and the interface between cells and the ECM can transduce mechanical stimuli to the cell (Galbraith et al., 2002). Integrin can bind to ECM proteins like fibronectin, which induces a conformational change in integrin that allows the binding of numerous intracellular proteins that form a complex called a focal adhesion. Downstream signalling of this

pathway eventually activates actin polymerization and cell migration (Zaidel-Bar et al., 2007). Most adherent cells not only can sense external forces, but they are also able to sample the mechanical properties of their extracellular matrix (ECM) and respond to its density, a process termed mechanotransduction (Discher et al., 2005). It is generally agreed that the linkage sites between cells and ECM are the local mechanosensors of adherent cells. They not only act as the pinning sites for adhesion, but also provide a platform for signal transduction. Despite growing knowledge about the molecular structure of adhesion sites, few studies have addressed how these anchorage points grow and how they sense the external forces. We propose that integrin mobility plays a key role in the regulation of the mechanosensing ability of an endothelial cell. This project investigates the role of integrin mobility and its ability to mechanosense external forces. To accomplish this, bovine arteriol endothelial cells (BAECs) were grown. The rate of recovery after photobleaching of fluorescently labelled integrin to a focal adhesion on various substrates of different rigidities and mechanical properties was then examined.

1.1 *Blood Vessels*

The vascular system is composed of the heart and vessels that carry blood towards and away from the heart. Arteries carry oxygenated blood and nutrients from the heart to the various organs and tissues of the body, while veins carry deoxygenated blood from tissues back to the heart. Capillaries are the tiny vessels in the body that allow the interchange of oxygenated blood and interstitial fluid between cells (Vascular system, 2008). The walls of the blood vessels are composed of a monolayer of endothelial cells. The endothelial cells rest on the basement membrane, a dense web of ECM proteins including laminin, collagen IV and fibronectin. Larger

vessels, such as veins and arteries, are also surrounded by a layer of smooth muscle cells. Outside the vessel are many adhesive proteins such as collagen I, III, V, VI that form a network called the interstitial matrix (Figure 2) (Strömblad & Cheresh, 1996).

1.2   Angiogenesis

Angiogenesis can be divided into three stages: initiation, proliferation and maturation. To initiate angiogenesis, signals such as VEGF or angiopoetin-2 (ANG-2) and chemokines released by hypoxic tumor or inflammatory cells stimulate endothelial cell proliferation. In response to ANG-2, vascular smooth muscle cells detach from the basement membrane of the vessel, releasing MMPs that degrade the surrounding ECM proteins (Carmeliet and Jain, 2011). Upon proteolysis of the ECM, growth factors, such as VEGF, are released by hypoxic, inflammatory or tumor cells which trigger cell proliferation and invasion (Strömblad & Cheresh, 1996). VEGF induces increased permeability between endothelial cells, allowing extravasation of proteins involved in the formation of a remodelled ECM scaffold. Integrin-mediated signalling leads to endothelial migration onto the remodelled ECM. One endothelial cell assumes the role of "tip" cell and its neighbors form a stalk, elongating the extension onto the ECM (Figure 3). In order to become a functional vessel, the extension forms a basement membrane by releasing tissue inhibitors of metalloproteinases (TIMPs) and plasminogen activator inhibitor-1 (PAI-1) (Carmeliet and Jain, 2011). Eventually, a closed loop is formed, facilitating blood flow (Carmeliet and Jain, 2011; Strömblad & Cheresh, 1996).

1.3   Hypoxia Induced Angiogenesis

Cancer cells contain the same range of molecules and pathways that normal cells have, but they differ in that there is aberrant regulation of key pathways, specifically cell growth. Cancer cells grow unchecked by normal growth regulators, proliferating into large collections of clonal cells, or tumors. As the tumor continues to grow without regulation, the microenvironment surrounding it becomes hypoxic, or depleted of oxygen, and deficient in nutrients (Andreef et al., 2000). Oxygen is needed for several essential metabolic pathways in mammalian cells including oxidative phosphorylation and energy metabolism. Thus, cancer cells cannot continue to divide without an oxygen supply. In order to adapt to this harsh environment, cancer cells are able to induce angiogenesis, while also resisting cell death (apoptosis) (Ruan et al., 2009). Under normal conditions, oxygen-sensing prolyl hydroxylase domain (PHD) proteins target hypoxia inducible factors (HIFs) for proteasomal degradation, the targeted breakdown of proteins (Ruan et al., 2009). Under hypoxic conditions, however, PHDs are inactive, which increases the concentration of HIFs within the cell, up regulating numerous hypoxia genes. HIF-α, for example, activates transcription of numerous angiogenic factors including VEGF, the VEGF receptor, SDF-1α and ANG-2 (Ruan et al., 2009; Carmeliet and Jain, 2011). SDF-1α binds at tip cells inducing angiogenesis proliferation (Carmeliet and Jain, 2011).

1.4   Integrin and the Extracellular Matrix

Integrin is a transmembrane heterodimer protein that is the interface between cells and their environment. The association of the α and β subunits forms an inactive dimer with two short cytoplasmic tails that can serve as a platform for numerous proteins upon activation (Galbraith et al., 2002). The integrin family can be broken

4

into several subclasses based upon the ligands they bind. For example, the integrin dimer we focus on in our studies is $\alpha_v\beta3$, which binds the three amino acid motif RGD (arginine, glycine, aspartate) found on ECM proteins such as fibronectin, fibrin, and von Willebrand factor (Brooks et al., 1994). During angiogenesis, integrins play a key role in sensing the mechanical properties of the ECM, adhering or inducing migration. Many studies have researched the dynamic relationship between integrin and the ECM and its role in cancer progression (Kaspar et al., 2006; Strömblad & Cheresh, 1996). By blocking the function of $\alpha_v\beta3$ integrin, vascular proliferation and tumor growth can also be inhibited (Hynes, 2007; Strömblad & Cheresh, 1996). Further insight into the mechanism behind this inhibition suggests an integrin-mediated "cytoprotective" effect of adhesion to the ECM (Buttery et al., 2004). The endothelial cells containing non-functional $\alpha_v\beta3$ integrins were not able to initiate angiogenesis, but instead died by apoptosis (Strömblad & Cheresh, 1996). Since tumor invasion involves numerous pathways including the directed migration of endothelial cells and the remodelling of the surrounding ECM proteins, understanding the relationship between integrin and the ECM is critical for developing new therapeutic treatments (Ruan et al., 2009).

1.5   Cell Migration

In response to mechanical or chemical stimuli, cells begin the migration process by taking on a polarized morphology. Cellular extensions, or pseudopodia, on the leading edge of the cell protrude as flat membrane structures with branched actin filaments (lamellipodia) and long narrow structures with parallel actin filaments (filopodia) (Le Clainche et al., 2008). Adhesions are formed between integrin and the ECM on the periphery of the lamellipodia, anchoring the protrusion. Integrin clusters in protein complexes called focal adhesions, connecting the ECM to the actin

5

cytoskeleton through a variety of proteins such as vinculin, talin and paxillin (Galbraith et al., 2002). Contraction of the actin bundles enables the cell to pull itself towards the focal adhesions at the leading edge, while also disassembling the adhesions at the lagging edge of the cell (Le Clainche et al., 2008).

1.6   Focal Adhesions

During cell migration, nascent focal adhesions within the pseudopodia at the leading edge of the cell make preliminary connections to the surrounding ECM, probing the extracellular environment (Wehrle-Haller & Imhof, 2002). These dynamic sites disassemble and reassemble at the periphery of the pseudopodia, a process termed adhesion turnover. Integrin is also a part to this dynamic quality, constantly diffusing in and out of focal adhesions, cycling between bound and unbound states (Ivaska, 2012). Nascent focal complexes contain β_3 integrin associated with adaptor proteins such as talin and paxillin. Talin activates integrin by binding to the cytoplasmic tail of the β subunit, while paxillin plays a role in scaffolding for other adaptor proteins leading to actomyosin involvement (Ivaska, 2012). Due to RhoA signalling, focal adhesions mature, recruiting $\alpha_v\beta3$ integrin along with vinculin, zxyin, FAK (focal adhesion kinase), and other phosphotyrosine proteins to the adhesion site (Figure 4) (Le Clainche et al., 2008). The recruitment of vinculin leads to a decrease in distance between the ECM and the cell creating a stronger adhesion. Studies have shown that this adhesion complex responds to internal and external forces (Galbraith et al., 2002; Wehrle-Haller & Imhof, 2002). Increased integrin endocytosis, calpain-mediated cleavage of talin and decreased tension are all known to increase focal adhesion disassembly (Ivaska, 2012).

1.7   Proposed Model of Integrin as a Mechanosensor

As endothelial cells migrate, they probe the pliability of their surroundings through focal adhesion complexes (Discher et al., 2005). It is has long been understood that cells can sense the mechanical properties of their environment and transduce this information to the rest of the cell, but the actual mechanisms behind this pathway are not completely elucidated (Wehrle-Haller & Imhof, 2002). We propose that integrin mobility plays a key role in the regulation of the mechanosensing ability of an endothelial cell. Studies have shown that epithelial cells, fibroblasts and neurons all react to the rigidity of their substrate, measured by a solid's elastic modulus E (Discher et al., 2005).   The elastic modulus is the mathematical description of a substance's propensity to be reversibly deformed when a force is applied. These cell lines, when seeded on soft gels with minimal cross-linking (E~1kPa), showed dynamic focal complexes, with weak adhesion properties. When these cells were seeded on densely cross-linked gels (E~ 50kPa), however, they contained stable, mature focal adhesions (Discher et al., 2005). We propose integrin mobility facilitates endothelial cells' ability to transduce the mechanical stimuli in the environment to adaptor proteins such as talin and paxillin (Figure 5). Tyrosine phosphorylation on many proteins involved in focal adhesion complexes, such as paxillin, has been shown to be greatly increased in cells on more rigid substrates. This phosphorylation event on paxillin correlates with an increase in the formation of mature focal adhesions. It has also been shown that induced actomyosin contraction leads to increased aggregation of integrin at focal adhesions, suggesting integrin's ability to sense the increased strain within the cell (Discher et al., 2005).

CHAPTER 2: MATERIALS AND METHODS

2.1 Cell Culture

Bovine aortic endothelial cells (BAECs) were cultured in Dulbecco's Modified Eagle Medium (DMEM)/Ham's Nutrient Mixture F12 (SAFC Biosciences; Lenexa, KS) enhanced with 10% fetal bovine serum (FBS; Thermo scientific; Logan, UT), 2mM L-glutamine and 1% penicillin/streptomycin antibiotics (GIBCO). Cells were passed at 70% confluence using 0.25% trypsin and 1mM EDTA in Hank's Salts (Thermo scientific; Logan, UT) for cell dissociation.

2.2 Transfection of Cells

Cultures of *E. coli* containing Alpha 5 Integrin-GFP (Addgene plasmid 15238) or Beta 3 Integrin-YFP (Addgene plasmid 26653) plasmids were inoculated on LB agar plates (0.01g/mL tryptone, 0.005g/mL yeast extract, 0.005g/mL NaCl; 0.018g/mL BactoAgar for agar plates) containing 30μg/mL kanamycin and incubated at 37°C. Isolated colonies were selected and used to inoculate 100mL LB broth containing 30μg/mL kanamycin. Cultures were grown overnight at 37°C while shaking at 130rpm. Cultures were centrifuged at 6800xg for 3 minutes. Pellets were resuspended and plasmid DNA was isolated using the QIAprep spin miniprep kit (Qiagen; Valencia, CA).

Prior to transfection, cells were grown to 95% confluence. Cell culture media was then removed and replaced with 5mL of serum free DMEM/ Ham's Nutrient Mixture F12 media. Cells were transfected with 8.0μg DNA (Alpha 5 Integrin-GFP or Beta 3 Integrin-YFP) and 21μL Lipofectamine 2000 (Invitrogen; Carlsbad, CA) for 4h at 37°C, 5% CO_2. After 4h, cell culture media was replaced with DMEM/Ham's

Nutrient Mixture F12 enhanced with 10% FBS. Following an incubation period of 24-48h, the cells were used for experiments.

2.3   Polyacrylamide Gel Preparation

Polyacrylamide gels were prepared in 14mm glass-bottomed petri dishes (MatTek; Ashland, MA). 250µL of 0.1M NaOH solution was added to the well of each petri dish and then placed on a hot plate at 80°C until all liquid evaporated leaving a crystalline coating. 50µL of 3-aminopropyl triethoxysilane (APES; Sigma-Aldrich; St. Louis, MO) was added to each NaOH coated well and allowed to sit for 20min with washings with distilled water at 5min intervals. 100µL of 0.5% glutaraldehyde (GIBCO) was added to the well of each petri dish and allowed to sit for 30min before aspirating off. 12mm glass coverslips were chloro-salinated by aliquoting 50µL of dichloromethylsilane (DCDMS; Sigma-Aldrich) onto each coverslip and then allowing it to sit for 5min. After 5min, each coverslip was rinsed until translucent with distilled water. The 40kPa gel solution was prepared with 200µL acrylamide, 240µL bis-acrylamide, and 560µL distilled water. The 8.7kPa gel solution was prepared with 125µL acrylamide, 150µL bis-acrylamide, and 725µL distilled water. 10% ammonium persulfate (AMPS; Sigma-Aldrich) was added to each gel solution at a 1:200 volume ratio and then allowed to de-gas in a vacuum chamber for 1h. After 1h, tetramethylethylenediamine (TEMED; Sigma-Aldrich) was added to each solution at a 1:2000 volume ratio and then vortexed for 5s before dispensing 4.5µL into the well of the amino-salinated petri dish. The chloro-salinated coverslip was then flipped over the gel solution, a metal bolt placed on top, aluminum foil wrapped around the dish and heated for 15min at 50°C. After 15min, the coverslip was removed and 3mL of distilled water was dispensed into each dish and allowed to sit for 15min with washings every 5min with distilled water. The gels

were then wrapped in parafilm and incubated at 37°C, 5% CO_2 overnight. After at least 10h, the gels were washed 3 times at 5min intervals with distilled water. Next, 250µL of 2mg/mL sulfo-SANPAH (Sigma-Aldrich) was aliquoted into the well of each petri dish and the dish was placed 3 inches from a UV lamp for 10min. The lid of the petri dish was sprayed with 70% ethanol and placed under the lamp as well. After 10min, each gel was washed 6 times with 50mM HEPES buffer (contains 11.92g/L HEPES; Sigma-Aldrich). The ligand used for Alpha 5 Integrin-GFP tests was fibronectin, while both fibronectin and vitronectin (Sigma-Aldrich) were used for Beta 3 Integrin-YFP tests. The stock solution of 10 µg/mL Rhodamine-tagged Fibronectin (Cytoskeleton, Inc.; Denver, CO) was diluted to 5 µg/mL with 50mM HEPES buffer. Vitronectin stock of 1mg/mL was diluted to 1µg/mL. Then, 95µL of the fibronectin or vitronectin solution was dispensed on top of each gel and incubated at 37°C, 5% CO_2 overnight.

2.4   Preparation of PA Gels with Fluorescent Beads

The same procedure was used to prepare the PA gels with fluorescent beads as noted above. After the gel solutions were allowed to degas for 1h in the vacuum, TEMED (Sigma-Aldrich) and 150µL of 2% solid carboxylate-modified Fluorosphere solution (Sigma-Aldrich) were added to each solution and vortexed for 10s. Both 1µm and 0.5µm diameter Fluorosphere beads were used in experiments. The gels were then prepared using the same procedure as above.

2.5   Seeding Cells on Polydimethylsiloxane(PDMS) Micro Posts

Transfected BAECs were washed 3 times with 1x phosphate buffered saline (PBS; 10x stock contains 85.0g/L NaCl, 1.8g/L NaH_2PO_4, and 12.35g/L Na_2PO_4). Cell dissociation was achieved using 0.25% trypsin and 1mM EDTA in Hank's Salts (Thermo scientific). The trypsin was quenched with DMEM/ Ham's Nutrient Mixture

F12 enhanced with 10% FBS (Thermo scientific; Logan, UT), 2mM L-glutamine and 1% penicillin/streptomycin antibiotics (GIBCO). The cell solution was centrifuged for 5 min in a VWR Clinical centrifuge at 3000rpm. The pellet was suspended in DMEM/ Ham's Nutrient Mixture F12 enhanced with 10% FBS (Thermo scientific; Logan, UT), 2mM L-glutamine and 1% penicillin/streptomycin antibiotics (GIBCO) and 1 mL of the cell solution was aliquoted onto the micro posts and incubated at 37°C, 5% CO_2 for 20 min. The media was removed from the dish and non-adherent cells were washed off with 5 washes with 1x PBS. 1mL of media was added and the cells were incubated at 37°C, 5% CO_2 overnight.

2.6   *Coating of PDMS Micro Posts with Fibronectin*

Fibronectin was diluted to a concentration of 5µg/mL using 50mM HEPES buffer (pH 7) for a final volume of 300µL. This solution was aliquoted onto the PDMS micro posts completely covering the posts in liquid. The dish was then incubated overnight at 37°C, 5% CO_2. The posts were washed 3 times with 1x PBS and cells were seeded using the protocol above.

2.7   *Seeding Cells on PA Gels*

Transfected BAEC cells were washed 3 times with 1x PBS. Cell dissociation was achieved using 0.25% trypsin and 1mM EDTA in Hank's Salts (Thermo scientific; Logan, UT). The trypsin was quenched with 3mL of DMEM/ Ham's Nutrient Mixture F12 enhanced with 10% FBS (Thermo scientific; Logan, UT), 2mM L-glutamine and 1% penicillin/streptomycin antibiotics (GIBCO) and then the cell solution was centrifuged for 5 min in VWR Clinical centrifuge at 3000rpm. The pellet was suspended in 6mL DMEM/ Ham's Nutrient Mixture F12 enhanced with 10% FBS (Thermo scientific; Logan, UT), 2mM L-glutamine and 1%

penicillin/streptomycin antibiotics (GIBCO) and 0.75mL of the cell solution was aliquoted onto each gel and incubated at 37°C, 5% CO_2 overnight.

2.8   FRAP of BAECs on PA Gel Substrates

Alpha 5 Integrin-GFP tagged BAECS were imaged using an Olympus Fluoview 1000 Laser Scanning Confocal Microscope with 400x and 1000x magnification. Isolated cells were chosen and FRAP was performed on single integrin clusters at focal adhesions along the periphery of the cell. The scanning laser 488nm was held at 15%. During photo-bleaching, the 488nm laser was held at 90%. A pre-bleach image, post-bleach and recovery images were taken for a total of 20 images over 80 seconds. The EGFP laser was held at 475 HV during the FRAP experiment. The bleached region of interest (ROI) was copied and pasted to a similar cluster away from the bleach on the same cell for a control. The ROI was also pasted to an area away from the bleach site where there were no cells for a background control.

2.9   FRAP of BAECs on Micro Post Substrates

Alpha 5 Integrin-GFP tagged BAECs were imaged using an Olympus Fluoview 1000 Laser Scanning Confocal Microscope at 40x and 100x objectives. The micro posts were visualized using Rhodamine Red X at 490 HV. Isolated cells were chosen and FRAP was performed on single integrin clusters at focal adhesions along the periphery of the cell where there was a noticeable deflection of the posts. The scanning laser 488nm was held at 15%. During photo-bleaching, the 488nm laser was held at 90%. A pre-bleach image, post-bleach and recovery images were taken for a total of 20 images over 80 seconds. The EGFP laser was held between 475 and 510 HV during the FRAP experiment. The bleached ROI was copied and pasted to a similar cluster away from the bleach on the same cell for a control. This ROI was

also pasted to an area away from the bleach site where there were no cells for a background control.

2.10   *FRAP of BAECs on PA Gels with Fluorescent Beads*

Alpha 5 Integrin-GFP tagged BAECs were imaged using an Olympus Fluoview 1000 Laser Scanning Confocal Microscope at 40x and 100x objectives. Isolated cells were chosen and FRAP was performed on single integrin clusters at focal adhesions along the periphery of the cell. The scanning laser 488nm was held at 15%. The fluorescent beads were visualized using Rhodamine Red X held at 490 HV. During photo-bleaching, the 488nm laser was held at 90%. A pre-bleach image, post-bleach and recovery images were taken for a total of 20 images over 80 seconds. The EGFP laser was held at 475 HV during the FRAP experiment. The bleached region of interest (ROI) was copied and pasted to a similar cluster away from the bleach on the same cell for a control. The ROI was also pasted to an area away from the bleach site where there were no cells for a background control. After the FRAP data was collected, the media was removed, without moving the plate. In order to dissociate the cells, 2mL of 0.25% trypsin and 1mM EDTA in Hank's Salts was aliquoted into the plate. After 5 minutes, the cell was imaged for any bead deformations.

2.11   *Analysis of FRAP Data*

The ROIs were selected and the FRAP data imported into Excel. For the micro posts, the area of the integrin cluster and the deflection of the micro posts determined using ImageJ software. Using Excel, the average fluorescent intensity of the background (F_{bgd}), unbleached control ($F_{control}$), and bleached (F_{bleach}) ROIs were determined. Using these values, the recovery curve was normalized (R_{norm}) to

account for loss of fluorescent molecules at focal adhesions due to bleaching and to correct for the fluorescence of the background using this formula:

$$R_{norm}= (F_{bleach}-F_{bgd})/(F_{control}-F_{bgd})$$

The fractional fluorescence recovery curve (R_{frac}) further corrected for post-bleach intensities (F_0) seen between 0.05 and 0.25 in the R_{norm} curve by setting the different post-bleach intensities to zero. The fractional fluorescent recovery curve was then determined by this formula:

$$R_{frac}= (R_{norm}-F_0)/(1-F_0)$$

The half maximal recovery time was then determined from this curve. The R_{frac} curves and $t_{1/2}$ of the hard and soft gels were compared, relating substrate rigidity to integrin recovery and focal adhesion stability.

2.12   Analysis of Cell Traction Force on Micro Posts

For the micro posts, the R_{frac} curves and $t_{1/2}$ of varying post heights were compared in order to relate substrate rigidity and integrin recovery. The deflection of the micro post (x), measured in Nikon software, was used to determine the traction force (F) exerted by the cell using this equation:

$$x= (64L^3F)/(3\pi ED^4)$$

E is the Young's Modulus for PDMS and is equal to 2.5 ± 0.5 MPa (Yang, et. al). D is the diameter of the micro posts (2µm) and L is the height of the micro post. The R_{frac} curves and cell traction force were compared.

2.13   Analysis of Cell Traction Force on PA Gels with Fluorescent Beads

The gels were originally constructed with a 1µm diameter bead concentration of 10-30µg/mL, which was increased to 150µg/mL. Fluorescent beads with a smaller

diameter of 0.5µm were also used. In order to calculate cell traction forces, we looked for distinct focal adhesions near numerous beads. In all of these experiments, the cells did not exhibit clear, distinct focal adhesions, limiting our ability to calculate cell traction forces.

2.13   *Alternative Integrin Subunit and Cell Line Test on Glass*

To test an alternative subunit of integrin and a different cell line, we transfected mouse melanoma B16 cells with Beta 3 Integrin-YFP and seeded them on glass, 10µg/mL fibronectin coated glass and 1µg/mL vitronectin coated glass. The cells were then observed on the Olympus Fluoview 1000 Laser Scanning Confocal Microscope.

CHAPTER 3: RESULTS

3.1   *Fluorescent Recovery was Quicker on a More Rigid PA Gel*

Fluorescent photo-bleaching of distinct focal adhesions in BAECs was performed (Figure 10). Following the bleaching event, the focal adhesions recovered fluorescence as bleached alpha 5 integrin-GFP diffused out and unbleached alpha 5 integrin-GFP diffused into the focal adhesion (Figure 9). BAECs plated on 40kPa PA gels showed a quicker and more complete alpha 5 integrin-GFP fluorescent recovery to bleached focal adhesions than cells plated on 8.7kPa PA gels (Figure 8, p= 0.05). The integrin recovery was quicker, reaching half-maximal intensity ($F\infty_{/2}$) in less time, when BAECs were seeded on the stiffer substrate (40kPa). For the 40kPa gels, $t_{1/2}$ was 30sec versus 36.65sec for the 8.7kPa gels (p=0.05, n=5). The relationship between substrate rigidity and integrin turnover was shown to be directly proportional (Figure 5).

3.2   Alpha 5 Integrin-GFP Clusters were not Distinct on PDMS Micro Posts

BAECs were plated on 9µm micro posts and post deflection was visualized (Figure 7). The micro posts were visualized using Rhodamine Red-X at 490 HV. The alpha 5 integrin fused GFP clusters were not localized and independent clusters (Figure 11, A). The proteins also often formed a ring around the post, instead of a solid cluster (Figure 11, B). The area of the cluster, therefore, was not measureable and could not be compared to the cell traction force. Since the clusters were not distinct, a fluorescent recovery curve for a single focal adhesion could not be determined.

3.3   Fibronectin Coating did not Improve Focal Adhesions

BAECs were plated on 9µm micro posts coated with 5µg/mL fibronectin and visualized on an Olympus Fluoview 1000 Laser Scanning Confocal Microscope. The integrin clusters looked similar to the previous micro post images. The focal adhesions were not distinct, lacking a defined boundary between adhesions (Figure 12, A). As seen in previous micro post tests, the integrin clusters formed a ring around the post (Figure 12, B). Fibronectin coating did not improve focal adhesion distribution.

3.4   Cell Traction Force and FRAP Analysis of BAECs on PDMS Micro Posts

BAECs transfected with alpha 5 integrin-GFP were seeded on PDMS micro pillar substrates and FRAP was recorded for focal adhesions near the periphery of the cell. The cells formed strong attachments to the posts, pulling the pillars away from their original position (Figure 7). The time each focal adhesion took to return to half-maximal fluorescence ($t_{1/2}$) was calculated and the mobile fraction (mf) of integrin molecules was determined. The deflection of the posts (x) due to cell adhesions was measured (Figure 7, B) and used to calculate the cell traction force with the equation

16

$x = (64L^3F)/(3\pi ED^4)$. The diameter (D) of each post is 2μm. The Young's Modulus (E) for PDMS is equal to 2.5 ± 0.5 MPa (Yang, et. al) (Figure 14, B). The length of the deflection of each pillar is directly proportional to the size of the cell traction force. While the trend is not significant ($R^2 = 0.3493$), there is a linear relationship between cell traction force and fluorescent recovery rate of integrin molecules to focal adhesions (Figure 14, A).

3.5   Cell Traction Force Determination from Fluorescent Bead Deformation

The gels were originally constructed using too low of a bead concentration (10-30μg/mL), which led to a very sparse number of beads near the focal adhesions (Figure 13, A). The bead concentration was increased to 150μg/mL, which led to a very blurred image due to an overlap of bead fluorescence (Figure 13, B). In the next experiment, fluorescent beads with a smaller diameter, 0.5μm, were added to the gels in order to minimize the overlap of fluorescence. In all of these experiments, the cells did not exhibit clear, distinct focal adhesions, limiting our ability to calculate cell traction forces.

3.6   Distinct Beta 3 Integrin Clusters were not Observed in B16 cells Seeded on Glass

To test an alternative subunit of integrin and a different cell line, transfected B16 cells with Beta 3 Integrin- YFP were seeded on glass, 10μg/mL fibronectin coated glass and 1μg/mL vitronectin coated glass. The fluorescence was dispersed throughout the entire cell, lacking any distinct regions of integrin clustering. This was observed on all three substrates.

CHAPTER 4: DISCUSSION

Angiogenesis requires the directed migration of the endothelial cells lining the nascent blood vessels. As endothelial cells begin to migrate during angiogenesis, they secrete matrix metalloproteinases (MMPs) to degrade the surrounding ECM (Carmeliet and Jain, 2011). This remodelling of the environment around the cell alters the density, or rigidity, of the cell's substrate, thus altering the mechanical stimuli to the surrounding cells. Integrin can transduce this mechanical stimulus to the cell (Galbraith et al., 2002). Various integrins, such as $\alpha_v\beta3$, are highly expressed on proliferating tumor blood vessels and are expressed at a much lower level on normal vessels (Garmy-Susini and Varner, 2008). An interaction between $\alpha_v\beta3$ integrin and MMP-2 activates MMP-2, thereby localizing its proteolytic activity to the invasive front of cells (Kryczka et al., 2012). Thus, the ECM closest to the leading edge of the cell is less dense then the ECM farther away from the cell. Most adherent cells not only can sense external forces, but they are also able to sample the mechanical properties of their substrate and respond to its density, a process termed mechanotransduction (Discher et al., 2005). Endothelial cells can sense the density gradient formed by the remodelled ECM and, therefore, migrate onto the newly formed ECM.

In order to migrate directionally, cells need to coordinate signalling pathways to generate cytoskeletal forces and control polarity (Stehbens and Wittmann, 2012). By dynamically altering adhesions sites to the ECM at the front and rear of the cell, cells can generate forces against its substrate. Integrin molecules are continuously internalized, shuttled to the leading edge of the cell, and incorporated into new focal adhesions (Gu et al., 2011). Small integrin clusters form at the leading edge of the cell. As the cell moves forward, these adhesions stay stationary with respect to the substrate. At the rear of the cell, retraction and sliding of focal adhesions requires a more compliant interaction with the substrate (Ballestrem et al., 2001).

Integrin can bind to ECM proteins like fibronectin, inducing a conformational change that allows the binding of numerous intracellular proteins that form a complex called a focal adhesion (Zaidel-Bar et al., 2007). RhoA signals through Rho-associated kinase (ROCK) to induce actin polymerization and stress fiber formation (Lamalice et al., 2007). Due to RhoA signalling, focal adhesions mature, recruiting $\alpha_v\beta3$ integrin along with vinculin, zxyin, and FAK to the adhesion site (Figure 4) (Le Clainche et al., 2008). FAK activates pathways known to promote cell proliferation. Integrin-stimulated phosphorylation of FAK forms a high affinity site that is recognized by several Src homology 2 (SH2) domain-containing proteins, including Src and Shc. Src links FAK to the Ras pathway via growth factor receptor-bound protein 2 (Grb2) (Provenzano and Keely, 2011). During proliferation, cells cannot progress through G1 into S phase in the absence of integrin-mediated adhesion, which appears to rely on Rho GTPases. Enhanced integrin-mediated signalling that occurs when cells are on stiff substrates will activate Rho GTPases and promote proliferation. Rho GTPases also have a role in inhibiting apoptosis, which might also contribute to cancer progression (Provenzano and Keely, 2011).

A rigid substratum such as glass resists intracellular contraction resulting in a distortion of the actin integrin linkage. This mechanical stress within the focal adhesion site generates a signal for actin polymerization and growth of the focal adhesion. In contrast, an elastic ECM substratum will not resist the acto-myosin–dependent focal adhesion contraction failing to generate a distortion signal that would enforce the focal adhesion. Thus, cells favor a rigid over an elastic substrate for adhesion (Ballestrem et al., 2001). In order to study focal adhesion dynamics related to force and substrate rigidity, we observed cells on three different substrates: PA gels, PDMS micro pillars, and PA gels embedded with fluorescent beads.

4.1   Substrate Rigidity Influences Integrin Diffusion

By seeding BAECs on two different gel rigidities, we were able to observe the role that integrin mobility plays in the regulation of the mechanosensing ability of an endothelial cell. The protocol for the formation of compliant gel substrates has been well established. One study estimates the width of these gels to be between 10-20µm (Aratyn-Schaus et al., 2010). In order to decrease this width and achieve a more uniform gel surface, we placed two metal washers on top of each gel during polymerization.

BAECs plated on more rigid 40kPa PA gels showed a quicker and more complete alpha 5 integrin fused GFP fluorescent recovery to bleached focal adhesions than cells plated on softer 8.7kPa PA gels (Figure 8, p= 0.05). When the BAECs were seeded on the more rigid substrate, they formed more stable focal adhesions. When observed on the softer substrate, however, the focal adhesions were smaller and less established. Studies have shown that epithelial cells, fibroblasts and neurons all react similarly to the rigidity of their substrate (Discher et al., 2005). These cell lines, when seeded on soft gels with minimal cross-linking (E~1kPa), showed dynamic focal complexes, with weak adhesion properties. When these cells were seeded on densely cross-linked gels (E~ 50kPa), however, they contained stable, mature focal adhesions (Discher et al., 2005). The relationship between substrate rigidity and integrin turnover correlates directly (Figure 5).

Integrin molecules diffuse through a cell's plasma membrane with seemingly Brownian motion, attaching and releasing attachments to receptors on the substrate. The weak short-range integrin-ligand bond opposes the generic interfacial repulsions between the cell and its substrate (Paszek et al., 2009). Large glycocalyx molecules are embedded in the plasma membrane, repulsing this integrin-ligand interaction due

to steric stress and electrostatic interactions (Paszek et al., 2009; Wehrle-Haller, 2012). On a soft, compliant substrate, such as the 8.7kPa gel, when integrin molecules bind to ligand molecules, the substrate is pulled closer to the cell at the attachment sites. This creates more room for the glycocalyx molecules, lessening the steric stress and favoring the integrin-ligand interaction (Figure 15, A). On a rigid substrate, such as the 40kPa gel, however, the substrate does not bend when attachments are formed, thus the steric stress is favored against the integrin-ligand interaction (Figure 15, B). Our data supports this model, in that on the softer substrate, the integrin turnover is slower because the integrin-ligand bond is energetically favored, retaining the integrin molecules in the focal adhesions longer. On the more rigid substrate, the integrin turnover is much faster due to the steric stress of the glycocalyx molecules. By altering the mechanical properties of a cell's substrate, it also affects its adhesive and migration tendencies.

4.2   *Alpha 5 Integrin-GFP FRAP and Cell Traction Force Assays*

Uniform arrays of cylindrical micro pillar substrates similar to those used in our studies have been utilized in order to study cell locomotion, focal adhesion dynamics and traction forces (Yang et al., 2011). The BAECs caused distinct deformations of micro posts due to adhesive and migration forces (Figure 7, A). This deflection can be easily visualized and measured in order to calculate cell traction force (Figure, B). Of the focal adhesions tested, many were stable mature adhesions with quick recovery rates and a limited number of mobile integrin molecules (Figure 14, A). While the trend between cell traction force and fluorescent recovery rate of integrin was not significant ($R^2 = 0.3493$), there is a linear relationship (Figure 14, B). A larger force correlates to less diffusion (longer $t_{1/2}$). When the formation of nascent adhesions is observed in the absence of force, the clustering of ligand bound integrins

and their association with adapter proteins such as talin, paxillin and FAK appears to be a diffusion driven process. As soon as tension is applied, however, vinculin is recruited and the connection to the actin cytoskeleton is stabilized (Wehrle-Haller, 2012). Thus, force stabilizes focal adhesions, energetically favoring the integrin-ligand interaction. This decreases the diffusion of the integrin molecules since they are retained more at adhesions.

The focal adhesions did not have distinct boundaries, thus we cannot determine if the recovery rates represent single adhesion sites. The deflection of the micro posts may also be due to more than one focal adhesion. The micro posts have fibronectin embedded in the tips of each post. We questioned whether this may have been degraded so we coated the micro posts with fibronectin as well. We observed the same issues as before: large clusters of focal adhesions and circular rings of integrin surrounding the posts (Figure 12). Cluzel et al. (2005) saw similar integrin clusters when β3-EGFP integrin-expressing B16F1 cells were seeded on micropatterned substrates with fibronectin/vitronectin. Perhaps, integrin molecules are continuously being cycled around the outer edge of the focal adhesion, thus the fluorescence is seen around the periphery.

Studies have shown that there is a linear relationship between the area of paxillin clusters at focal adhesions and the cell traction force exerted. The slope of this trend is about $5nN/\mu m^2$ (Balaban et al., 2001). Perhaps expression of a different recombinant integrin protein may yield better results, enabling an investigation of whether another integrin isoform would exhibit this same trend.

4.3   Cell Traction Force Determination from Fluorescent Bead Deformation

Several studies have employed fluorescent beads in order to test cell traction forces exerted by cells (Discher et al., 2005). The deformation of the substrate due to cell-generated stresses can be detected based on the displacement of embedded fluorescent beads near the substrate surface. Images of the beads before and after cell detachment by treatment with 0.25% trypsin were obtained and analyzed for bead displacement. The shift is normally less than 1μm (Lo et al., 2000).   By increasing the bead concentration from 10μg/mL to 150μg/mL, the proportion of beads to cells was improved. This, however, caused an issue with the diffuse fluorescence of the beads (Figure 13). By using a smaller diameter bead, 0.5μm, the images improved. Similar to the micro post experiments, no defined focal adhesions in the cells were observed. If the best integrin DNA construct can be determined in order to observe distinct focal adhesions, cell traction force tests can be performed on either micro post substrates or PA gels embedded with fluorescent beads.

4.4   Distinct Beta 3 Integrin Clusters were Not Observed in B16 Cells Seeded on Glass

To improve the quality of the focal adhesion clusters observed, an alternate recombinant integrin protein was transfected into B16 cells. Numerous migration and focal adhesion studies utilize B16 cells and beta 3 integrin (Ballestrem et al., 2001). When beta 3 integrin-YFP transfected B16 cells were plated on glass, fibronectin coated glass and vitronectin coated glass, the YFP fluorescence was diffuse throughout the cells in each test. There were no discreet areas of integrin clusters near focal adhesions. The plasmid was obtained from Addgene, which sequenced the construct 3 times. To verify the sequence, however, we are going to sequence the construct ourselves. If it contains a deletion or error, this would cause the production of a non-functional protein. Further analysis must be done in order to determine if the

plasmid is the right sequence for beta 3 integrin-YFP. Once this is determined, the best ligand for tests must also be decided since beta 3 integrin attaches to both fibronectin and vitronectin.

4.5   Concluding Remarks

The fluorescent recovery results from the different rigidity PA gel tests support our original hypothesis that integrin mobility plays a key role in the regulation of the mechanosensing ability of an endothelial cell. By monitoring the recycling of integrin to adhesion sites, these studies elucidated that cells exhibited more stable focal adhesions on more rigid substrates and more dynamic nascent adhesions on softer substrates. Tests could be done on a serial range of rigidities in order to further refine this data. The protocols established for cell traction force assays on PDMS micro posts and PA gels embedded with fluorescent beads can serve as a baseline for future studies. A linear trend was observed between cell traction force and rate of recovery of fluorescent integrin molecules. Additional tests can be done in order to supplement this data. If a suitable recombinant integrin protein can be expressed in either B16 or BAEC cells, both the micro posts and the PA gels embedded with fluorescent beads can be utilized to determine cell traction forces of focal adhesions. The stress exerted on the substrate by the cell can be compared with integrin recovery to bleached focal adhesions, further revealing the role integrin plays in mechanotransduction.

CHAPTER 5: REFERENCES

Andreeff M, Goodrich DW, Pardee AB. Cell Proliferation, Differentiation, and Apoptosis. In: Bast RC Jr, Kufe DW, Pollock RE, et al., editors. Holland-Frei Cancer Medicine. 5th edition. Hamilton (ON): BC Decker; 2000. Chapter 2. Available from: http://www.ncbi.nlm.nih.gov/books/NBK20860/

Aratyn-Schaus Y., Oakes P.W., Stricker J., Winter S.P., Gardel M.L. (2010). Preparation of Complaint Matrices for Quantifying Cellular Contraction. JoVE. http://www.jove.com/index/Details.stp?ID=2173, doi: 10.3791/2173

Balaban, et al. (2001). Force and focal adhesion assembly: a close relationship studied using elastic micropatterned substrates. Nature Cell Biology, 3, 466-472.

Ballestrem et al. (2001). Marching at the Front and Dragging Behind: differential $\alpha v\beta 3$ turnover regulates focal adhesion behavior. Journal of Cell Biology, 155 (7), 1319-1332.

Brooks, P.C., Clark, R.A., & Cheresh, D.A. (1994). Requirement of Vascular Integrin Alpha v Beta 3 for Angiogenesis. Science, 264, 569-571.

Buttery, R., Rintoul, R., & Sethi, T. (2004). Small Cell Lung Cancer: The Importance of the Extracellular Matrix. The International Journal of Biochemistry and Cell Biology, 36, 1154-1160.

Carmeliet, P., & Jain, R.K. (2011). Molecular Mechanisms and Clinical Applications of Angiogenesis. Nature, 473, 298-307.

Cheng, Q., et al. (2010). Flexible Micropost Arrays for Studying Traction Forces of Vascular Smooth Muscle Cells. CBMS, 1904-906.

Cluzel, C., Saltel, F., Lussi, J., Paulhe, F., Imhof, F., and Wehrle-Haller, B. (2005). The mechanisms and dynamics of $\alpha_v\beta_3$ Integrin clustering in living cells. Journal of Cell Biology, 171(2), 383-392.

Discher, D.E., P. Janmey, and Y.L. Wang (2005). Tissue cells feel and respond to the stiffness of their substrate. Science, 310(5751), 1139-43.

Galbraith, C., Yamada, K. and Sheetz, M. (2002). The relationship between force and focal complex development. Journal of Cell Biology, 159, 695-705.

Garmy-Susini and Varner. (2008). The Role of Integrins in Tumor Angiogenesis and Lymphangiogenesis. Lymphatic Research and Biology, 6, 155-163.

Gu, Z., E.H. Noss, V.W. Hsu, and M.B. Brenner. 2011. Integrins traffic rapidly via circular dorsal ruffles and macropinocytosis during stimulatedcell migration. J. Cell Biol. 193:61–70. http://dx.doi.org/10.1083/jcb.201007003

Hynes, R.O. (2007). Cell-Matrix Adhesion in Vascular Development. Journal of Thrombosis and Maemostatis, 5, 32-40.

Insall, R.H. (2010). Understanding Eukaryotic Chemotaxis: A Pseudopod-Centered View. Nature Reviews Molecular Cell Biology, 11, 453-458.

Ivaska, Johanna. (2012). Unanchoring Integrins in Focal Adhesions. Nature Cell Biology, 14, 981-983.

Kaspar, M., Zardi, L., & Neri, D. (2006). Fibronectin as Target for Tumor Therapy. International Journal of Cancer, 118, 1331-1339.

Kryczka, J., Stasiak, M., Dziki, L., Mik, M., Dziki, A., and Cierniewski, C. (2012). The Journal of Biological Chemistry, 287, 36556–36566.

Lamalice, L., Le Boeuf, F., & Huot, J. (2007). Endothelial Cell Migration During Angiogenesis. Circulation Research, 100, 782-794.

Le Clainche & Carlier. (2008). Regulation of Actin Assembly Associated With Protrusion and Adhesion in Cell Migration. Physiological Reviews, 88, 489–513.

Li, B., Xie, L., Starr, Z., Yang, Z., Lin, J., & Wang, J. (2007). Development of Micropost Force Sensor Array with Culture Experiments for Determination of Cell Traction Forces. Cell Motility and the Cytoskeleton, 64, 509-518.

Lo et al. (2000). Cell Movement Is Guided by the Rigidity of the Substrate. Biophysical Journal, 79, 144-152.

Millard, M., Odde, S., & Neamati, N. (2011).Integrin Targeted Therapeutics. Theranostics, 1, 154-188.

Paszek, M., Boettiger, D., Weaver, V., Hammer, D. (2009). Integrin Clustering Is Driven by Mechanical Resistance from the Glycocalyx and the Substrate. PLoS Comput Biol 5(12): e1000604. doi:10.1371/journal.pcbi.1000604

Provenzano, P. and Keely, P. (2011). Mechanical signaling through the cytoskeleton regulates cell proliferation by coordinated focal adhesion and Rho GTPase signalling. Journal of Cell Science, 124, 1195-1205.

Ruan, K., Song, G., & Ouyang, G. (2009). Role of Hypoxia in the Hallmarks of Human Cancer. Journal of Cellular Biochemistry, 107, 1053-1062.

Stehbens, S. and Wittmann, T. (2012). Targeting and Transport: How Microtubules control focal adhesion dynamics. Journal of Cellular Biology, 198, 481–489.

Strõmblad, S., & Cheresh, D.A. (1996). Cell Adhesion and Angiogenesis. Trends in Cell Biology, 6, 462-468.

Swaney, K. F., Huang, C. H. & Devreotes, P. N. (2010). Eukaryotic chemotaxis: a network of signaling pathways controls motility, directional sensing, and polarity. Annual Review of Biophysics, 39, 265-89.

Vascular System. NewYork-Presbyterian Hospital, Nov. 2008. Web. 06 Dec. 2012. <http://nyp.org/health/cardiac-overvasc.html>.

Wehrle-Haller, B. (2012). Assembly and Disassembly of Cell Matrix Adhesions. Current Opinion in Cell Biology, 24, 569-581.

Wehrle-Haller, B. & Imhof, B.A. (2002). The Inner Lives of Focal Adhesions. Trends in Cell Biology, 12, 382-389.

Yang, et al. (2011). Assaying Stem Cell Mechanobiology on Microfabricated Elastomeric Substrates with Geometrically Modulated Rigidity. Nature Protocol 6 (2), 187-213.
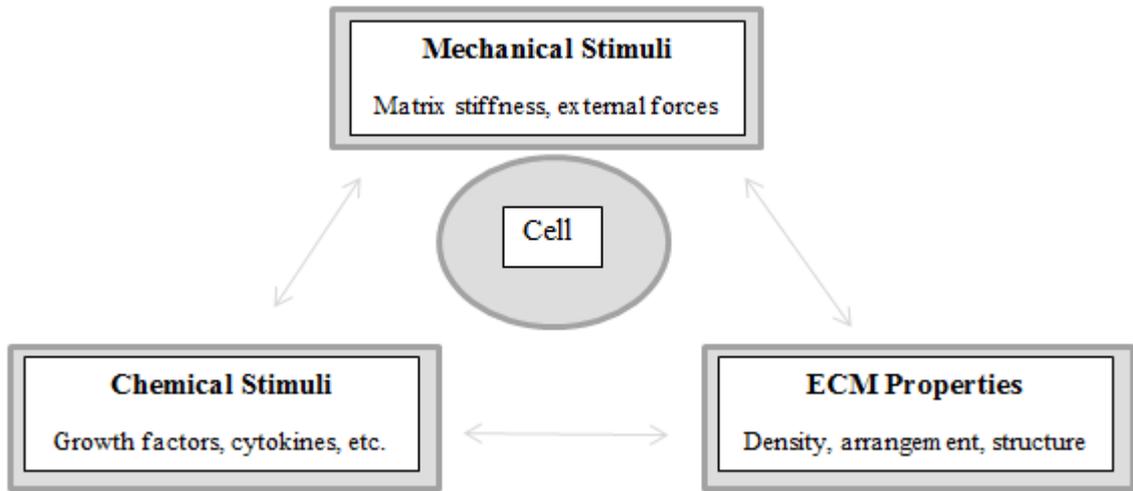
Image adapted from Provenzano and Keely (2011)

Figure 1- **Regulators of a Cell's Microenvironment.** The primary factors in a cell's microenvironment that influence migration and adhesion are chemical and mechanical stimuli and the structure of the surrounding extra-cellular matrix (ECM).
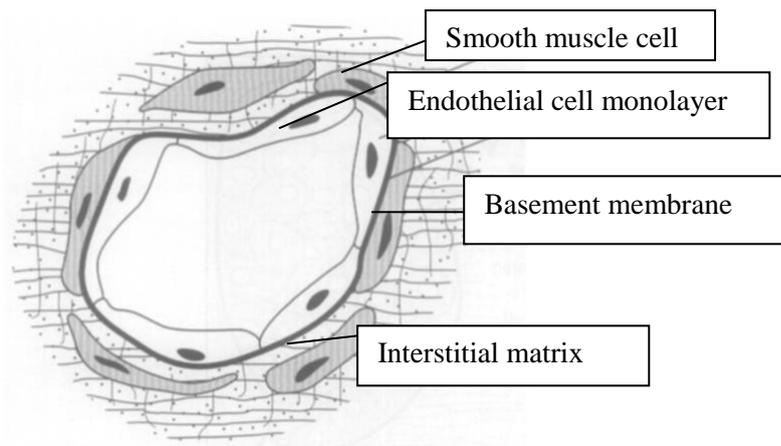
Image adapted from StrÖmblad and Cheresh (1996)

Figure 2- **Schematic of the Structure of a Blood Vessel.** The lining of a blood vessel consists of endothelial cells lying on top of a basement membrane. Larger vessels also have smooth muscle cells surrounding the endothelial cells. The interstitial matrix is a network of extra-cellular matrix proteins that encompass the vessel.

Permeability, extravasation and vasodilation

Tip formation (integrins) and angiogenic factors (VEGF)

Matrix remodeling (matrix metalloproteinases)

Flow
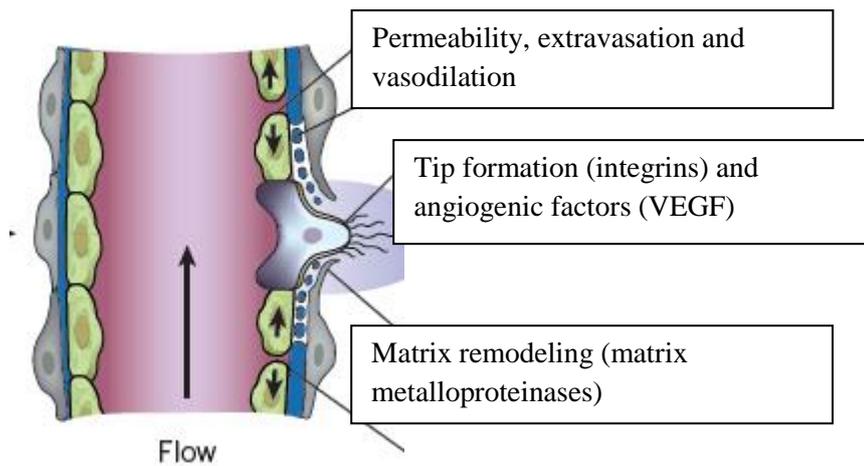
Image adapted from Carmeliet and Jain (2011)

Figure 3- **Initiation of Angiogenesis.** Elongation of blood vessels begins with selection and formation of a tip cell, increased permeability of the vessel, and degradation of the basement membrane by metalloproteases. This allows extravasation of proteins such as fibronectin that remodel the surrounding interstitial matrix, facilitating endothelial cell migration.
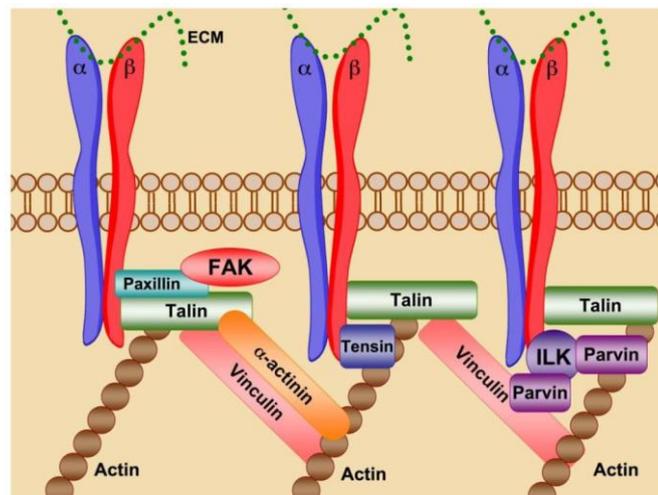
Image adapted from Millard et al. (2011)

Figure 4- **Focal Adhesion Complexes.** Cells adhere to the ECM through protein complexes called focal adhesions. Integrins bind to fibronectin through an "RGD" motif. This bonding allows integrin to transduce the mechanical signals from the environment to proteins within the cell. Focal adhesion kinase (FAK) unfolds in response to mechanical force, leading to a phosphorylation of paxillin and recruitment of actin-bound talin. Activated beta integrin cytoplasmic tails bind talin, promoting cytoskeleton assembly via the crosslinking of both vinculin and actin. The association of talin with vinculin can lead to cell contraction and recruitment of other focal adhesion complexes.

Figure 5- **Effects of Substrate Rigidity on Integrin Turnover**. A stiffer, more rigid substrate correlates to a higher traction force on the cell. In this situation, focal adhesions are more stable and integrin turnover increases. When seeded on a softer substrate, cells exhibit more dynamic integrin clusters in nascent focal complexes.
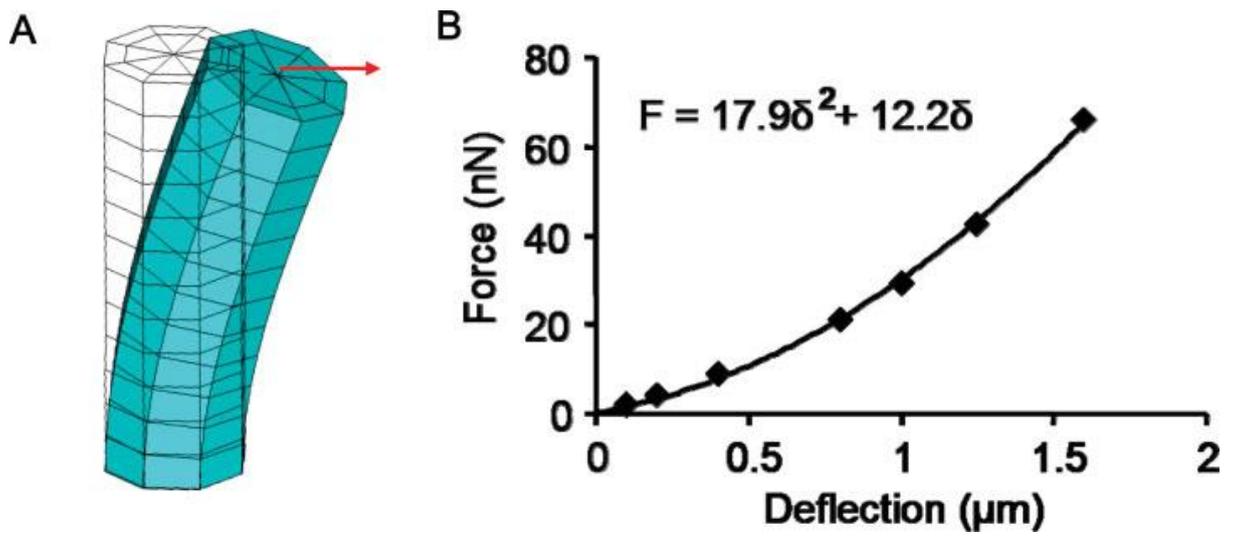
$$F = 17.9\delta^2 + 12.2\delta$$

Image adapted from Li et al. (2007)

Figure 6- **Use of Micro Post Substrates for Cell Traction Force Arrays.** Cells can be seeded on top of polydimethylsiloxane micro posts. A) As the cells develop stable adhesions, they pull the posts away from their original positions. This cell traction force can be determined by a deflection measurement. B) A shorter post correlates to a more rigid substrate, while a longer post represents a softer substrate.
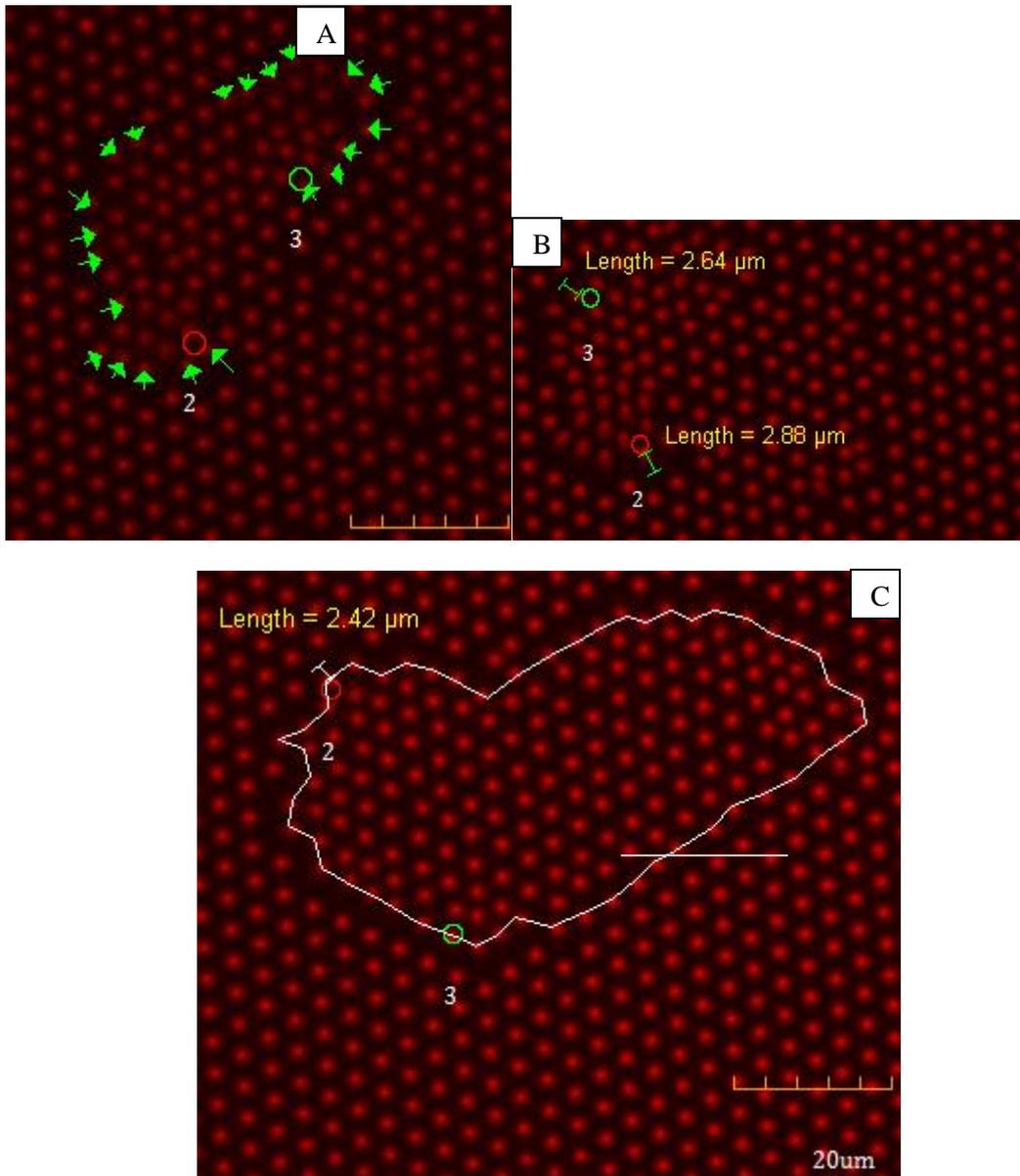
Figure 7- **Fluorescent Recovery After Photo-bleaching on 9μm Micro Posts.** The micro posts are visualized with Rhodamine Red-X 490 HV. The region of interest (ROI) denoted 2 is the bleached focal adhesion, while 3 is a control. The scale bar is 20μm. The deflection of the posts due to the cell traction forces can be easily seen from the cell outline (C) and arrows showing the movement of the posts (A). The length of the deflection is directly proportional to the size of the force exerted by the cell (B).
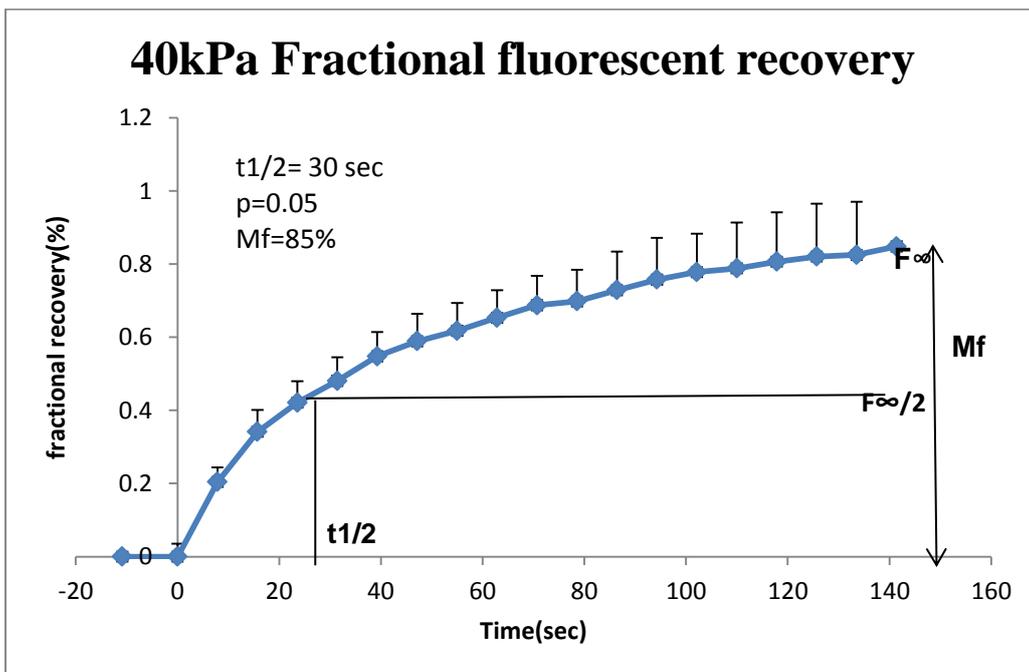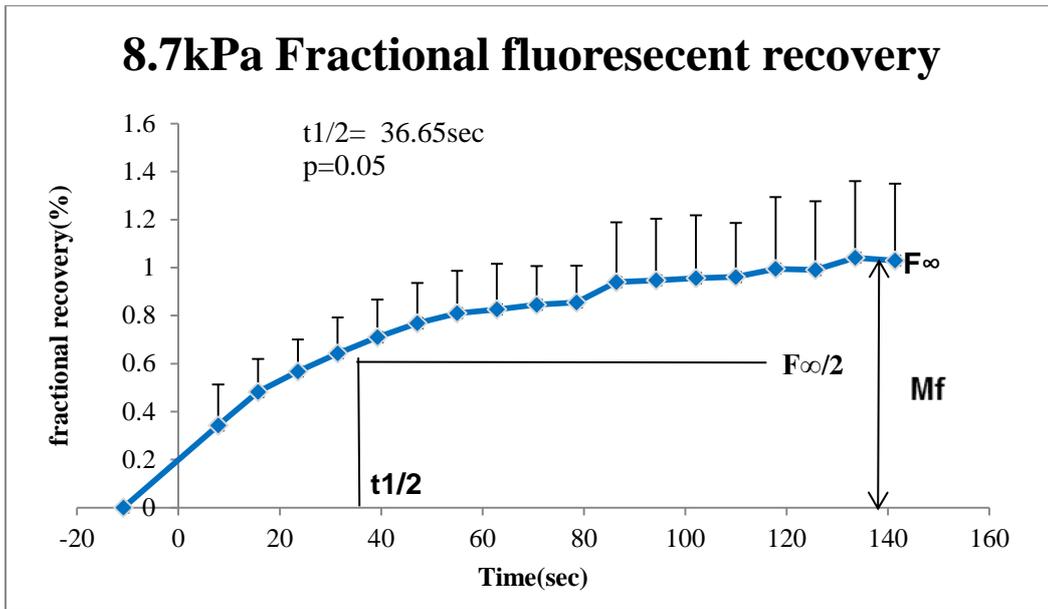
Figure 8- **Fractional Fluorescent Recovery of Alpha 5 Integrin-GFP on 8.7kPa and 40kPa Polyacrylamide Gels.** 8.7kPa or 40kPa denotes the crosslinking density of the gel. 8.7kPa is the "soft" substrate here, while 40kPa is the "rigid" substrate. The fractional recovery curve was calculated by accounting for control focal adhesion bleaching and background intensities. Five sets of data (n=5) were averaged in order to standardize the data. The fractional recovery curve allows direct extraction of the mobile fraction (Mf) and $t_{1/2}$. The integrin recovery was quicker, reaching half-maximal intensity ($F\infty_{/2}$) in less time, when cells were seeded on the stiffer substrate.
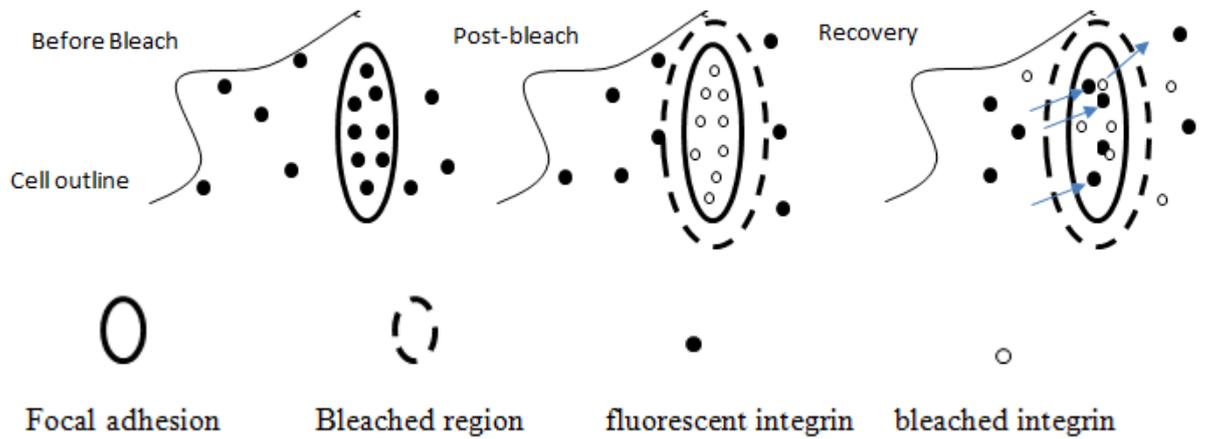
Figure 9- **Schematic of Fluorescent Inactivation and the recovery process of GFP-tagged integrins to focal adhesions.** In a hypothetical cell, fluorescent integrin molecules are clustered in focal adhesion complexes near the periphery of cells (left image). Right after photo-bleaching, the bleached integrin molecules remain concentrated in the focal adhesion (center image). With time, the fluorescent molecules exchange for bleached integrin molecules, prompting a fluorescent recovery within the focal adhesion.
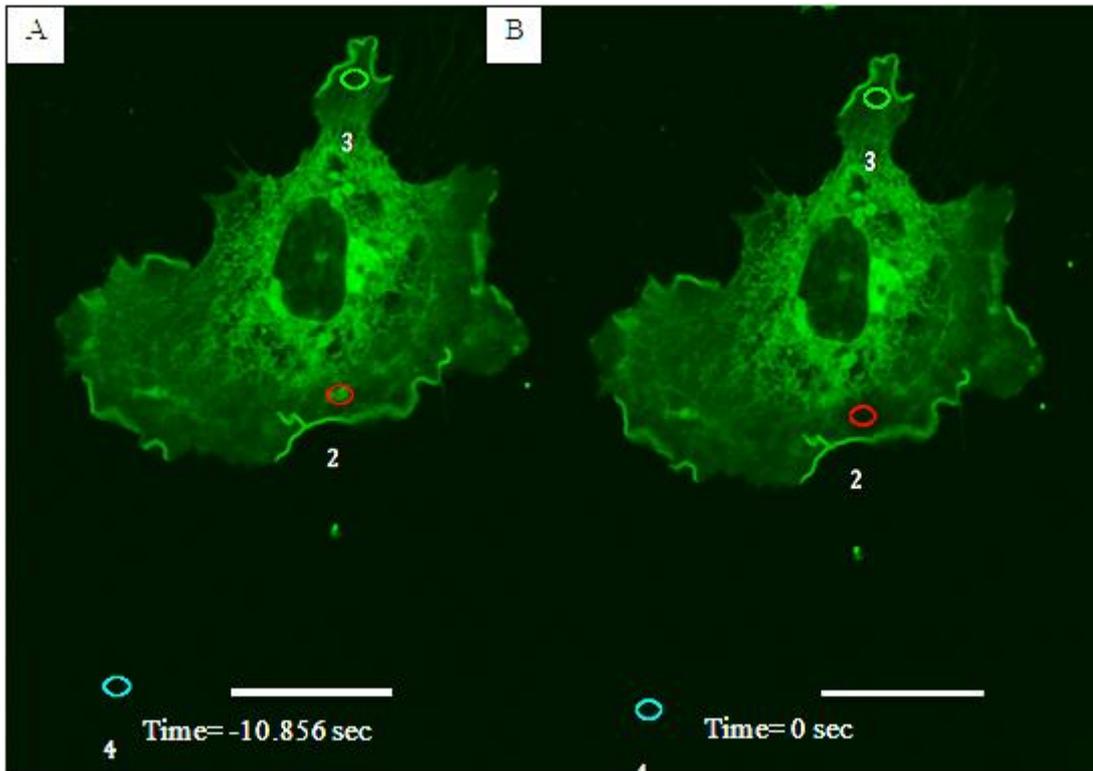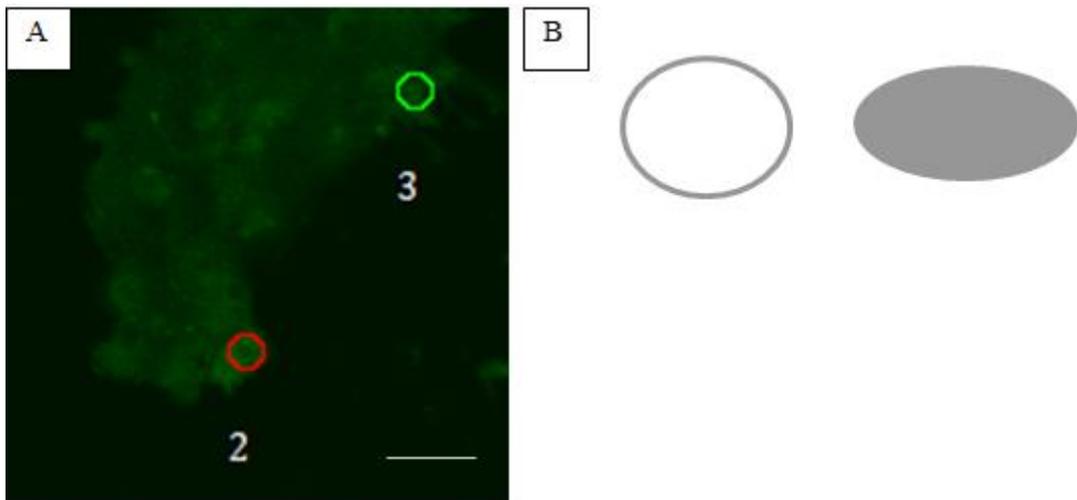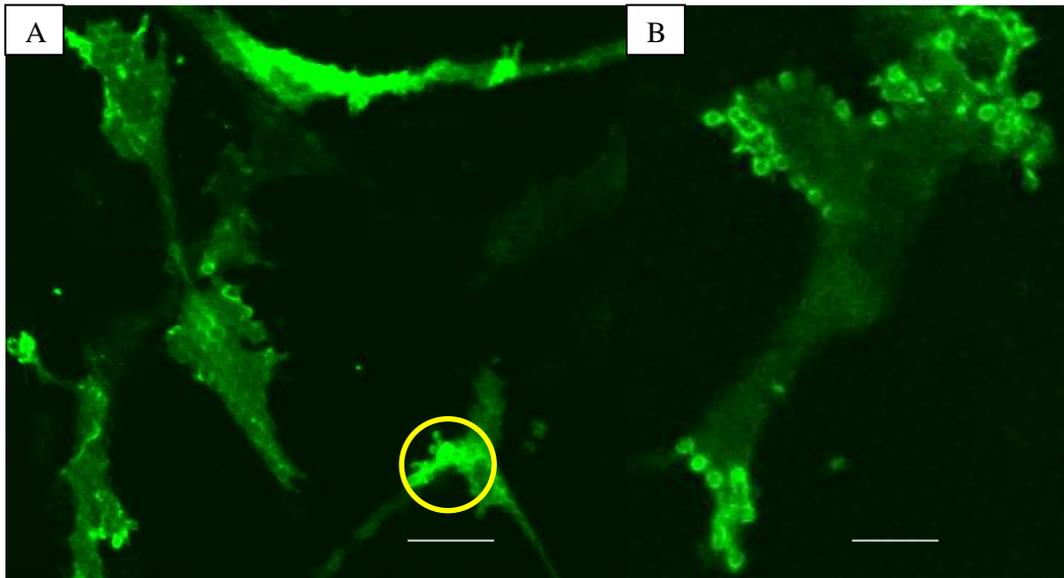
Figure 10- **Bovine Arteriol Endothelial Cells Transfected with Alpha 5 Integrin-GFP.** The endothelial cell was seeded on 40kPa polyacrylamide gel. The scale bar corresponds to 20μm. A) The cell before photo-bleaching. B) The cell post-bleach. ROI 2 denotes the distinct focal adhesion of interest, while 3 and 4 are bleach and background controls.

Figure 11- **Clustered Focal Adhesions in Bovine Arteriol Endothelial Cells Plated on 9μm Micro Post.** The endothelial cell was transfected with Alpha 5 Integrin fused GFP and plated on a 9μm micropost. The scale bar is 20μm. The 2 denotes the focal adhesion to be bleached and the 3 denotes a control. A) The integrin clusters were not distinct and independent . B) The clusters were often found in a ring form, encircling the post, instead of a solid cluster. The area of the clusters, therefore, were not measurable, and thus, could not be compared to the cell traction force.

Figure 12- **Bovine Arteriol Endothelial Cell Plated on Fibronectin Coated 9μm Micro Posts.** The endothelial cells were transfected with alpha 5 integrin fused GFP and plated on 9μm micro posts. The posts are made with fibronectin on the tips of each post, but in order to try to improve the quality of the observed focal adhesions, the posts were coated with an additional 5μg/mL of fibronectin. The scale bar is 20μm. A) The focal adhesions do not contain any distinct boundaries. B) This single cell contains numerous adhesion sites where integrin has clustered. The focal adhesions, however, encircle the posts in a ring instead of forming solid clusters. This is the same issue seen when the cells were seeded on the micro posts before adding fibronectin.
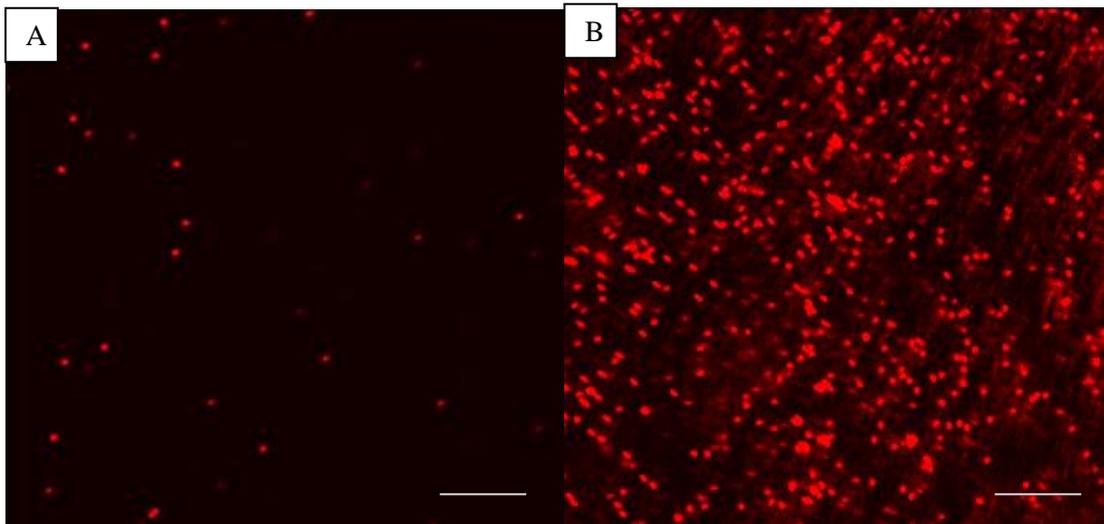
Figure 13- **Polyacrylamide Gels Embedded with Fluorescent Beads.** A) The polyacrylamide gel was prepared with 30µg/mL of 1µm diameter fluorescent beads. There are not enough beads present in order to perform cell traction force experiments. B) The polyacrylamide gel was prepared with 150µg/mL of 1µm diameter fluorescent beads. There are a sufficient number of beads in order to perform cell traction force experiments, but the fluorescence from the beads is spread out.

Cell Traction Force and Fluorescent Recovery Rate on Micro Posts

$y = 2.8108x + 134.95$
$R^2 = 0.3493$
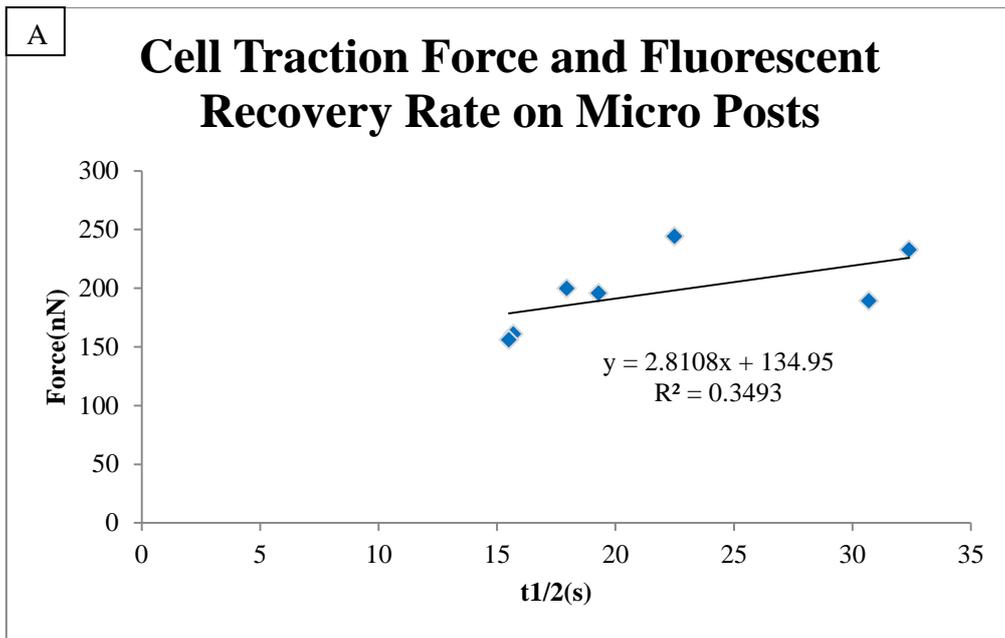
Deflection	Force (nN)	t1/2 (s)	mf(%)
1.99	160.7964017	15.7	43
2.34	189.0771759	30.7	21
1.93	155.948269	15.5	74
3.02	244.02268	22.5	45
2.42	195.5413529	19.3	41
2.88	232.7103704	32.4	140
2.47	199.5814635	17.95	31

Figure 14- **Cell Traction Force Determination from PDMS Micro Post FRAP Tests.** BAECs transfected with alpha 5 integrin-GFP were seeded on 9μm PDMS micro pillar substrates. Focal adhesions were photo-bleached and the fluorescent recovery was monitored. A) There was no significant trend found between $t_{1/2}$ and the cell traction force measurements. B) The time each focal adhesion took to return to half-maximal fluorescence ($t_{1/2}$) was calculated and the mobile fraction (mf) of integrin molecules was determined. The deflection of the posts (x) due to cell adhesions was measured and used to calculate the cell traction force (F) with the equation $x = (64L^3F)/(3\pi ED^4)$. The diameter (D) of each post is 2μm. The length (L) of the micro posts is 9μm. The Young's Modulus (E) for PDMS is equal to 2.5 ± 0.5 MPa (Yang, et. al).
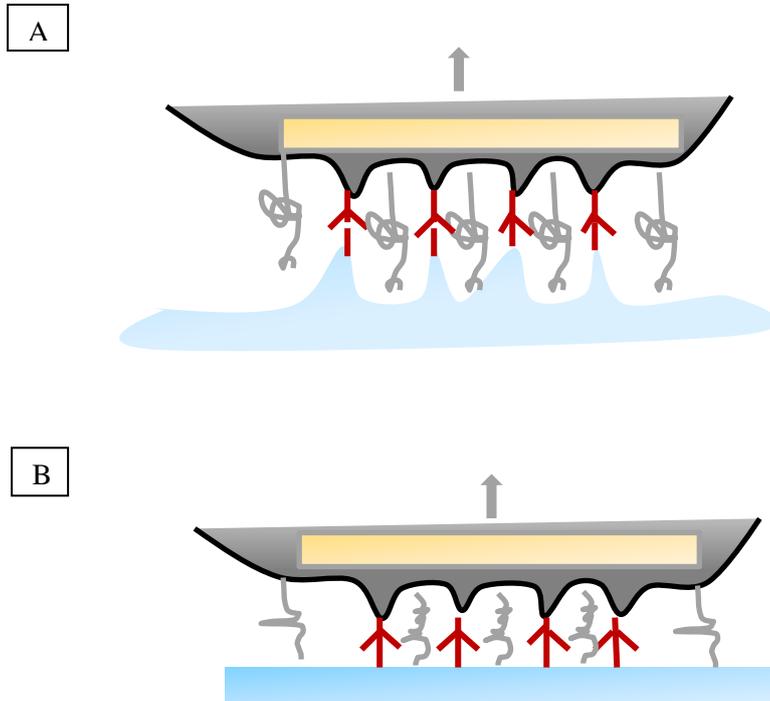
Figure 15- **Schematic Representation of an Adhesion Cluster on a Compliant and Rigid Substrate.** The mobile integrin molecules in the cell membrane (gray) can form specific bonds with ligand proteins on the substrate (blue). Oligosaccharides form a network called the glycocalyx which produces an interfacial steric and electrostatic repulsion. A) On a soft substrate, the substrate and membrane deform in response to contractile forces within the cell. This eases the steric compression of the gylocalyx molecules. B) On a rigid substrate, the substrate does not deform in response to contractile forces within the cell. There is a larger steric repulsion between the cell membrane and the substrate.

BIOGRAPHY OF THE AUTHOR

From the day she was born on October 14, 1990, Jennifer MacDowell has been a passionate and determined individual. Whether it was in the pool, in the gym, or on the field, she spent her childhood competing. When she wasn't playing sports, she was exploring the great outdoors, searching for salamanders and building forts. Her ten years of participation in Destination Imagination taught her lessons in problem solving, creativity, and out-of-the-box thinking. She found her true passion, however, in science. After graduating high school in 2009, she chose to become a UMaine black bear. She spent her four years at Maine studying biochemistry and representing her school on the softball team. While she will be venturing on to Tufts Medical School in the fall, she will always keep a warm place for the college of her heart always.